7. Y. Onodera *et al.*, *Cell* **120**, 613 (2005).
8. J. Penterman *et al.*, *Proc. Natl. Acad. Sci. U.S.A.* **104**, 6752 (2007).
9. R. Lister *et al.*, *Cell* **133**, 523 (2008).
10. X. Zhang, Y. V. Bernatavichute, S. Cokus, M. Pellegrini, S. E. Jacobsen, *Genome Biol.* **10**, R62 (2009).
11. A. Kirmizis *et al.*, *Nature* **449**, 928 (2007).

Acknowledgments: This work was supported by National Institutes of Health grants R01GM070795 and R01GM059138 to J.-K.Z. and by the Chinese Academy of Sciences (CAS), China. We thank B. Stevenson for technical assistance and X. Zhang for the gift of glutathione *S*-transferase H3 (amino acids 1 to 57) construct. Sequence data are available in the Gene Expression Omnibus database (GEO accession GSE33071).

Supplementary Materials
www.sciencemag.org/cgi/content/full/336/6087/1445/DC1
Materials and Methods
Figs. S1 to S17
Tables S1 to S7
References (*12*–*20*)

20 January 2012; accepted 26 April 2012
10.1126/science.1219416

MORC Family ATPases Required for Heterochromatin Condensation and Gene Silencing

Guillaume Moissiard,[1] Shawn J. Cokus,[1] Joshua Cary,[1] Suhua Feng,[1] Allison C. Billi,[2] Hume Stroud,[1] Dylan Husmann,[1] Ye Zhan,[3] Bryan R. Lajoie,[3] Rachel Patton McCord,[3] Christopher J. Hale,[1] Wei Feng,[4] Scott D. Michaels,[4] Alison R. Frand,[5] Matteo Pellegrini,[1,6] Job Dekker,[3] John K. Kim,[2] Steven E. Jacobsen[1,5,6,7]*

Transposable elements (TEs) and DNA repeats are commonly targeted by DNA and histone methylation to achieve epigenetic gene silencing. We isolated mutations in two *Arabidopsis* genes, *AtMORC1* and *AtMORC6*, which cause derepression of DNA-methylated genes and TEs but no losses of DNA or histone methylation. AtMORC1 and AtMORC6 are members of the conserved *Microrchidia* (*MORC*) adenosine triphosphatase (ATPase) family, which are predicted to catalyze alterations in chromosome superstructure. The *atmorc1* and *atmorc6* mutants show decondensation of pericentromeric heterochromatin, increased interaction of pericentromeric regions with the rest of the genome, and transcriptional defects that are largely restricted to loci residing in pericentromeric regions. Knockdown of the single MORC homolog in *Caenorhabditis elegans* also impairs transgene silencing. We propose that the MORC ATPases are conserved regulators of gene silencing in eukaryotes.

Gene silencing in the *Arabidopsis* genome is highly correlated with DNA methylation, which is found in three different cytosine contexts. Methylation of symmetric CG and CHG sites (in which H is A, T, or C) are mediated by DNA METHYLTRANSFERASE1 (MET1) and CHROMOMETHYLASE3 (CMT3), respectively, whereas CHH methylation is mainly catalyzed by DOMAINS REARRANGED METHYLTRANSFERASE2 (DRM2) (*1*). Silent loci are also enriched in the repressive histone H3 lysine 9 dimethylation mark (H3K9me2) (*2*, *3*).

Suppressor of drm2 cmt3 (*SDC*) is a gene whose repression in most tissues depends on the redundant activities of DRM2 and CMT3 (*4*, *5*). Hence, a loss of *SDC* silencing is observed in the *drm2 cmt3* double mutant but not in *drm2* or *cmt3*

[1]Department of Molecular, Cell, and Developmental Biology, University of California at Los Angeles, Terasaki Life Sciences Building, 610 Charles Young Drive East, Los Angeles, CA 90095–723905, USA. [2]Life Sciences Institute and Department of Human Genetics, University of Michigan, Ann Arbor, MI 48109, USA. [3]Lazare Research Building 570N, Program in Systems Biology and Gene Function and Expression, University of Massachusetts Medical School, 364 Plantation Street, Worcester, MA 01605, USA. [4]Department of Biology, Indiana University, Bloomington, IN 47405, USA. [5]Department of Biological Chemistry, David Geffen School of Medicine, University of California Los Angeles, Los Angeles, CA 90095, USA. [6]Eli and Edythe Broad Center of Regenerative Medicine and Stem Cell Research, University of California Los Angeles, Los Angeles, CA 90095, USA. [7]Howard Hughes Medical Institute, University of California Los Angeles, Los Angeles, CA 90095, USA.

*To whom correspondence should be addressed. E-mail: jacobsen@ucla.edu

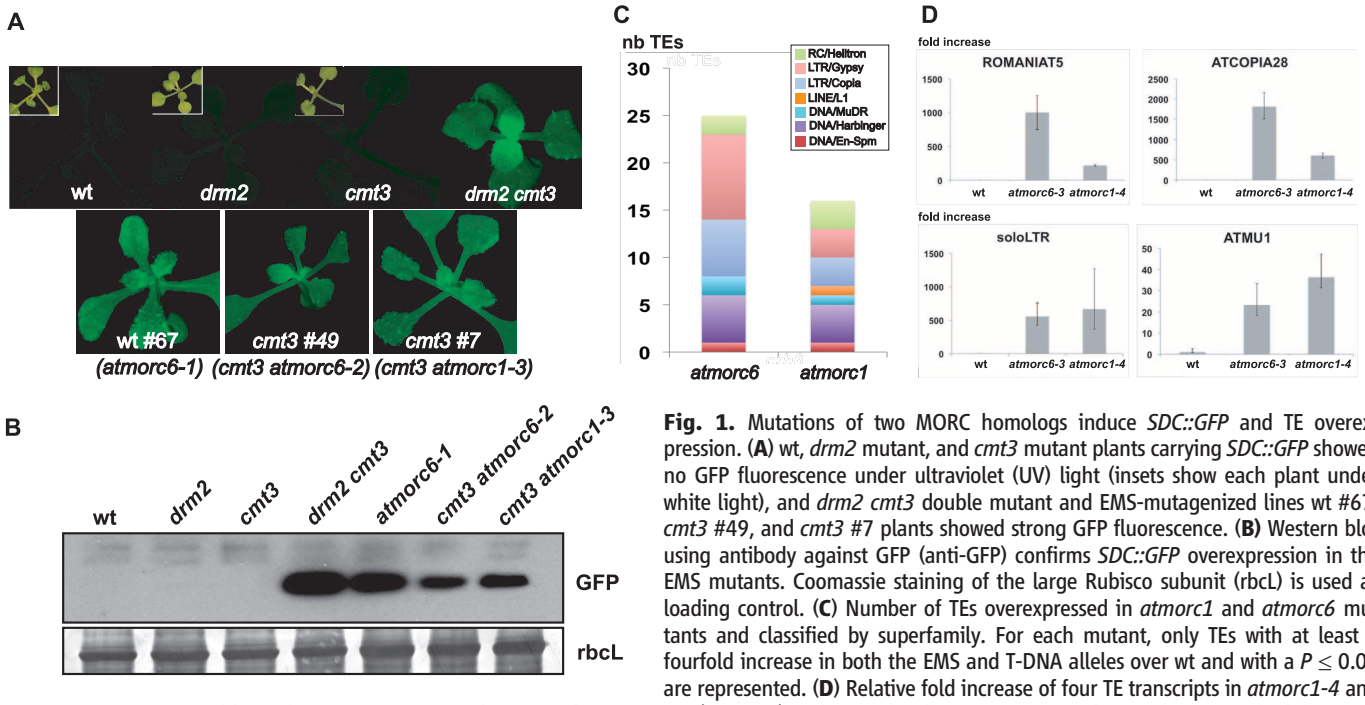

Fig. 1. Mutations of two MORC homologs induce *SDC::GFP* and TE overexpression. (**A**) wt, *drm2* mutant, and *cmt3* mutant plants carrying *SDC::GFP* showed no GFP fluorescence under ultraviolet (UV) light (insets show each plant under white light), and *drm2 cmt3* double mutant and EMS-mutagenized lines wt #67, *cmt3* #49, and *cmt3* #7 plants showed strong GFP fluorescence. (**B**) Western blot using antibody against GFP (anti-GFP) confirms *SDC::GFP* overexpression in the EMS mutants. Coomassie staining of the large Rubisco subunit (rbcL) is used as loading control. (**C**) Number of TEs overexpressed in *atmorc1* and *atmorc6* mutants and classified by superfamily. For each mutant, only TEs with at least a fourfold increase in both the EMS and T-DNA alleles over wt and with a $P \leq 0.05$ are represented. (**D**) Relative fold increase of four TE transcripts in *atmorc1-4* and *atmorc6-3* over wt assayed by real-time quantitative polymerase chain reaction (RT-qPCR) and normalized to *ACTIN7*. Errors bars indicate standard deviation based on three independent biological replicates.

single mutants. The *SDC* promoter carries seven tandem repeats, which recruit the DNA methylation machinery and cause transcriptional gene silencing. We engineered a green fluorescent protein (GFP)–based sensor construct controlled by the *SDC* promoter (fig. S1A). The *SDC::GFP* transgene behaves similarly to endogenous *SDC*, and GFP fluorescence is not detectable in wild-type, *drm2*, or *cmt3* plants but is highly expressed in *drm2 cmt3* double mutant (Fig. 1A).

We carried out ethyl methanesulfonate (EMS) mutagenesis screens in wild-type (wt) or *cmt3* backgrounds for mutants showing *SDC::GFP* overexpression and identified the wt #67, *cmt3* #7, and *cmt3* #49 mutants (Fig. 1, A and B). Mapping experiments using bulk segregant analysis coupled to deep genome resequencing indicated that *cmt3* #7 contained a mutation in *At4g36290* (*AtMORC1*), previously also named *COMPROMISED RECOGNITION OF TCV-1* (*CRT1*) (*6*, *7*), whereas wt #67 and *cmt3* #49 both contained mutations in *At1g19100* (*AtMORC6*) (*7*) (figs. S1B, S2, and S3A). An *atmorc1* allele was previously reported to show reduced resistance to

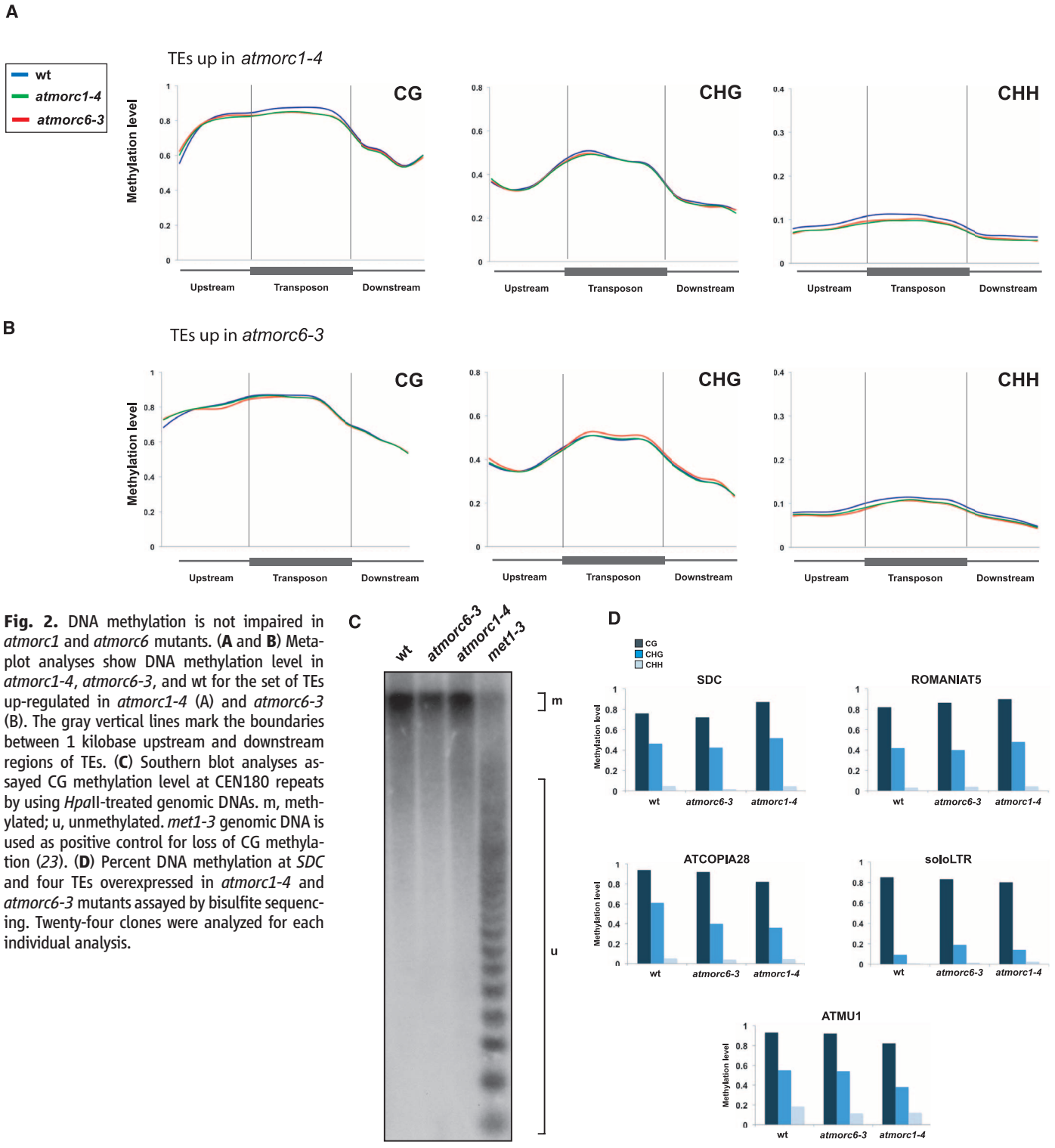

Fig. 2. DNA methylation is not impaired in *atmorc1* and *atmorc6* mutants. (**A** and **B**) Metaplot analyses show DNA methylation level in *atmorc1-4*, *atmorc6-3*, and wt for the set of TEs up-regulated in *atmorc1-4* (A) and *atmorc6-3* (B). The gray vertical lines mark the boundaries between 1 kilobase upstream and downstream regions of TEs. (**C**) Southern blot analyses assayed CG methylation level at CEN180 repeats by using *Hpa*II-treated genomic DNAs. m, methylated; u, unmethylated. *met1-3* genomic DNA is used as positive control for loss of CG methylation (*23*). (**D**) Percent DNA methylation at *SDC* and four TEs overexpressed in *atmorc1-4* and *atmorc6-3* mutants assayed by bisulfite sequencing. Twenty-four clones were analyzed for each individual analysis.

the turnip crinkle virus (TCV) (*6*, *7*), suggesting that AtMORC1 is involved in viral resistance in addition to its role in gene silencing described in this study, whereas mutations in *AtMORC6* have not been described. To ensure that *atmorc1* and *atmorc6* mutations were those responsible for the loss of *SDC* silencing, we isolated knock-out transferred DNA (T-DNA) insertion lines *atmorc1-4* and *atmorc6-3* and confirmed *SDC* overexpression in these two mutant alleles (fig. S3, B to D). Genetic complementation crosses between the recessive EMS and T-DNA mutants confirmed *AtMORC1* and *AtMORC6* as the mutated genes responsible for *SDC::GFP* activation in the three EMS lines (fig. S3E). Therefore, #7, #67, and #49 were renamed *atmorc1-3*, *atmorc6-1*, and *atmorc6-2*, respectively.

By using RNA sequencing (RNA-seq) (*8*), we found that the majority of RNAs significantly affected in the *atmorc1* and *atmorc6* mutants showed up-regulation, and many of these were transposable elements (TEs) belonging to various transposon superfamilies, including, among others, the LTR/Gypsy, LTR/Copia, DNA/MuDR, and DNA/Harbinger families (Fig. 1, C and D; fig. S4A; table S1). The expression defects in the *atmorc1* and *atmorc6* mutants were very similar, with all but two of the transposons up-regulated in *atmorc1* also up-regulated in *atmorc6* (fig. S4B). Protein-coding genes overexpressed in the *atmorc1* and *atmorc6* EMS and T-DNA mutants included endogenous *SDC* (table S2). There was a high degree of overlap between the genes up-regulated in *atmorc1* and *atmorc6* (fig. S4C), most of them corresponding to DNA-methylated and silenced loci (fig. S4, D and E). We also performed RNA-seq in the *atmorc1 atmorc6* double mutant and found a very similar set of genes and transposons up-regulated, with only a few genes up-regulated in the double mutant that were not up-regulated in each of the single mutants (table S3), suggesting that AtMORC1 and AtMORC6 may act together to enforce gene silencing.

Whole-genome bisulfite sequencing (BS-seq) (*9*) revealed that DNA methylation levels in all sequence contexts were unaltered in *atmorc1* or *atmorc6* relative to wild type at TEs up-regulated in *atmorc1* or *atmorc6* (Fig. 2, A and B), nor were there any bulk alterations in protein-coding genes or TEs in the genome (fig. S5, A and B). In addition, analyses at the pericentromeric satellite CEN180 repeats and five loci up-regulated in *atmorc1* and *atmorc6* showed that the DNA methylation patterns in *atmorc1-4* and *atmorc6-3* were similar to those of wild type (Fig. 2, C and D). Chromatin immunoprecipitation sequencing (ChIP-seq) analyses of H3K9me2 also did not reveal any changes in the *atmorc1* or *atmorc6* mutants at *SDC* or other up-regulated locations (fig. S6, A and B). Lastly, small RNA sequencing analyses showed that elements up-regulated in *atmorc1* and *atmorc6* mutants were enriched in small interfering RNAs (siRNAs), but these siRNA levels did not change in the mutants (fig. S7). Thus, *AtMORC1* and *AtMORC6* are not required to maintain DNA methylation, H3K9me2, or siRNAs, suggesting that AtMORC1 and AtMORC6 are likely to either act downstream of DNA methylation or enforce silencing by a novel mechanism.

AtMORC1 and *AtMORC6* are homologs of mouse *Microrchidia1* (*MORC1*) (*10*, *11*) and contain gyrase, Hsp90, histidine kinase, and MutL (GHKL) and S5 domains, together comprising an adenosine triphosphatase (ATPase) module (*6*) in addition to a putative C-terminal coiled-coil domain (fig. S1B). The EMS mutations found in *atmorc1-3*, *atmorc6-1*, and *atmorc6-2* alleles all introduced premature stop codons within the GHKL domain (fig. S1B).

Because of the similarity of AtMORC1 and AtMORC6 to ATPases involved in manipulating chromatin superstructure (*12*), these proteins may affect gene silencing through higher-order compaction of methylated and silent chromatin. In wild-type nuclei, pericentromeric heterochromatin forms densely staining nuclear bodies called chromocenters that localize to the nuclear periphery

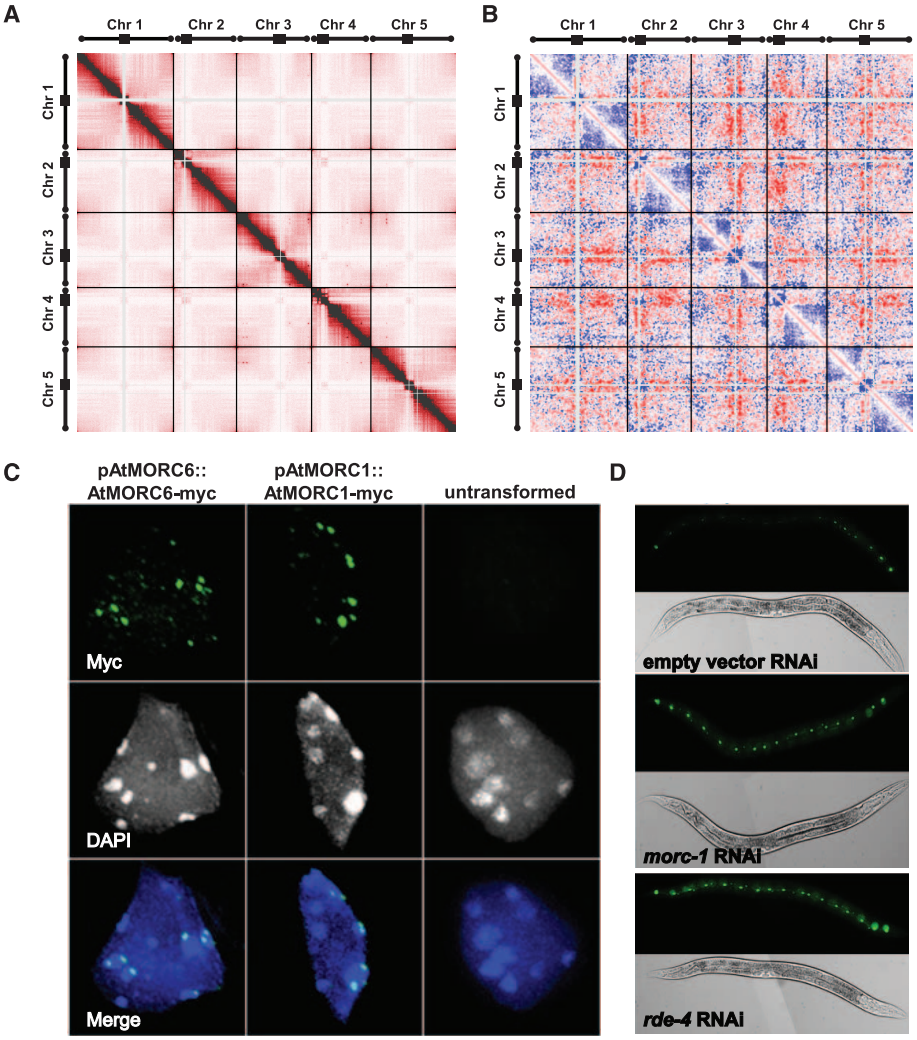

Fig. 3. AtMORC1 and AtMORC6 are required for maintenance of chromatin architecture and form nuclear bodies near chromocenters, and *morc-1* is involved in gene silencing in *C. elegans*. (**A**) Interaction matrix of the wt *Arabidopsis* genome from Hi-C analysis. Positions along the five chromosomes are shown from left to right and top to bottom, and each pixel represents interactions from uniquely mapping paired end reads in 200-kilobase bins. Black bars and circles mark the positions of the pericentromeric and telomeric regions, respectively. Light gray regions represent areas masked out because of problematic mapping. Black bars show separation between chromosomes. (**B**) Difference plot shows enrichment of Hi-C interactions in *atmorc6-1* in red and interactions depleted in *atmorc6-1* in blue. (**C**) Anti-Myc immunostaining showing localization of pAtMORC6::AtMORC6-Myc and pAtMORC1::AtMORC1-Myc in nuclear bodies adjacent to chromocenters. AtMORC1 and AtMORC6 showed 2.0 ± 1.0 (average ± standard deviation) and 2.5 ± 1.2 bodies per chromocenter, respectively. DAPI (4′,6-diamidino-2-phenylindole) staining shows chromocenter location. Bottom images are merges. (**D**) A silenced seam cell–specific GFP transgene in the *eri-1* (*mg366*) sensitized background is overexpressed in worms fed with bacteria expressing double-stranded RNA targeting *morc-1* or *rde-4* but not in worms fed with bacteria expressing a control empty vector. Results are representative of five independent replicates.

(*13*). We observed decondensation of chromocenters in the *atmorc1* and *atmorc6* mutants (as well as in *atmorc1 atmorc6* double mutant) (figs. S8 to S11) and found that loci transcriptionally derepressed in the mutants mostly localized to pericentromeric heterochromatin (fig. S12 and tables S1 and S3). To directly examine whole-genome chromatin interactions, we performed Hi-C analyses in wild type and *atmorc6-1* (*14*). Consistent with previous cytological studies (*13*), the wild-type genome showed interactions between telomeres as well as between euchromatic regions on the same chromosome arm (Fig. 3A). In contrast, pericentromeric heterochromatin regions interacted very weakly with the rest of the genome, consistent with their compaction in chromocenters (Fig. 3A). Although *atmorc6-1* showed a roughly similar chromatin architecture (fig. S13), plotting the differences between mutant and wild type showed that *atmorc6-1* shows an increase in interactions between the pericentromeric regions of all chromosomes with the euchromatic arms of all chromosomes and a corresponding depletion of interactions of euchromatic arms with themselves. Because the analysis reports relative changes with the sum of differences set to zero, the most likely interpretation of these findings is that pericentromeric regions interact more strongly with the euchromatic arms in *atmorc6-1*, although we cannot exclude that the mutant also has effects on the euchromatic arms (Fig. 3B). This interpretation is consistent with the cytological observations showing that chromocenters expand out into a larger area of the nucleus in the mutants (fig. S8). We also found, by using complementing myc-tagged transgenes, that AtMORC1 and AtMORC6 proteins formed small nuclear bodies that were usually adjacent to but not within chromocenters (Fig. 3C and figs. S14 and S15). These results are all consistent with a model in which AtMORC1 and AtMORC6 enforce compaction and gene silencing of pericentromeric heterochromatin, although it is also possible that changes in chromatin and gene expression in the mutant secondarily lead to the observed changes in chromatin compaction. Mutation of the plant-specific *MOM1* gene has also been shown to affect gene silencing but not DNA methylation in *Arabidopsis*; however, *mom1* mutants do not show chromocenter decondensation and therefore are likely to act via a different mechanism (*15*, *16*).

A single MORC homolog, *morc-1*, is present in the worm *Caenorhabditis elegans*, which is devoid of DNA methylation (*17*). To test whether the *C. elegans morc-1* (ZC155.3) is involved in gene silencing, we performed RNA interference (RNAi)–mediated knockdown of *morc-1* in the *eri-1* sensitized background, in which a GFP transgene is silenced in most of the worm seam cells (Fig. 3D) (*18*). *morc-1*–depleted worms showed GFP reactivation similar to worms depleted of *rde-4*, an essential component of gene silencing in *C. elegans* (Fig. 3D) (*19*). These results suggest that MORCs may play an ancient and conserved role in gene silencing. In addition, the observation that *morc-1* is required for gene silencing in *C. elegans* reinforces our view that MORCs in *Arabidopsis* are enforcing silencing by a mechanism that may not be directly linked with DNA methylation. It is interesting to note that the phenotype of the *Morc1*-knockout mouse resembles *Miwi2*- and *Dnmt3L*-knockout mouse phenotypes, showing male-specific meiotic defects during spermatogenesis (*10*, *20*–*22*). Miwi2 and Dnmt3L are both required for TE silencing, and it is possible that Morc1 might be involved in transposon silencing in mammals as well. We propose that MORC family ATPases act to regulate chromatin architecture and gene silencing in a wide variety of eukaryotes.

References and Notes

1. J. A. Law, S. E. Jacobsen, *Nat. Rev. Genet.* **11**, 204 (2010).
2. J. P. Jackson, A. M. Lindroth, X. Cao, S. E. Jacobsen, *Nature* **416**, 556 (2002).
3. F. Malagnac, L. Bartee, J. Bender, *EMBO J.* **21**, 6842 (2002).
4. X. Zhang *et al.*, *Cell* **126**, 1189 (2006).
5. I. R. Henderson, S. E. Jacobsen, *Genes Dev.* **22**, 1597 (2008).
6. H. G. Kang, J. C. Kuhl, P. Kachroo, D. F. Klessig, *Cell Host Microbe* **3**, 48 (2008).
7. H. G. Kang *et al.*, *Plant Cell* **22**, 918 (2010).
8. Z. Wang, M. Gerstein, M. Snyder, *Nat. Rev. Genet.* **10**, 57 (2009).
9. S. J. Cokus *et al.*, *Nature* **452**, 215 (2008).
10. M. L. Watson *et al.*, *Proc. Natl. Acad. Sci. U.S.A.* **95**, 14361 (1998).
11. N. Inoue *et al.*, *Hum. Mol. Genet.* **8**, 1201 (1999).
12. L. M. Iyer, S. Abhiman, L. Aravind, *Biol. Direct* **3**, 8 (2008).
13. P. Fransz, J. H. De Jong, M. Lysak, M. R. Castiglione, I. Schubert, *Proc. Natl. Acad. Sci. U.S.A.* **99**, 14584 (2002).
14. E. Lieberman-Aiden *et al.*, *Science* **326**, 289 (2009).
15. P. Amedeo, Y. Habu, K. Afsar, O. Mittelsten Scheid, J. Paszkowski, *Nature* **405**, 203 (2000).
16. A. V. Probst, P. F. Fransz, J. Paszkowski, O. Mittelsten Scheid, *Plant J.* **33**, 743 (2003).
17. V. J. Simpson, T. E. Johnson, R. F. Hammen, *Nucleic Acids Res.* **14**, 6711 (1986).
18. S. Kennedy, D. Wang, G. Ruvkun, *Nature* **427**, 645 (2004).
19. H. Tabara *et al.*, *Cell* **99**, 123 (1999).
20. M. A. Carmell *et al.*, *Dev. Cell* **12**, 503 (2007).
21. D. Bourc'his, T. H. Bestor, *Nature* **431**, 96 (2004).
22. A. A. Aravin *et al.*, *Mol. Cell* **31**, 785 (2008).
23. M. W. Kankel *et al.*, *Genetics* **163**, 1109 (2003).

Acknowledgments: We thank M. Akhavan for sequencing, L. Goddard and L. Iruela-Arispe for assistance with confocal microscopy, and P. Fransz and I. Schubert for helpful discussions. S.F. is a Special Fellow of the Leukemia and Lymphoma Society. J.C. is supported by the Ruth L. Kirschstein National Research Service Award GM007185. R.P.M. is supported by the National Institute of General Medical Sciences (grant F32GM100617), and J.D. is supported by a W. M. Keck Foundation Distinguished Young Scholar in Medical Research Award. Research in the Jacobsen, Kim, Michaels, and Dekker laboratories was supported by NIH grants GM60398, GM088565, GM075060, and HG003143, respectively. Sequencing files have been deposited at Gene Expression Omnibus (GEO) (accession code GSE37644). The authors declare no competing financial interests. S.E.J. is an investigator of the Howard Hughes Medical Institute. Correspondence and requests for materials should be addressed to S.E.J.

Supplementary Materials

www.sciencemag.org/cgi/content/full/science.1221472/DC1
Materials and Methods
Figs. S1 to S15
Tables S1 to S4
References (*24*–*44*)

5 March 2012; accepted 24 April 2012
Published online 3 May 2012;
10.1126/science.1221472

The Structures of COPI-Coated Vesicles Reveal Alternate Coatomer Conformations and Interactions

Marco Faini,[1] Simone Prinz,[1] Rainer Beck,[2] Martin Schorb,[1] James D. Riches,[1]* Kirsten Bacia,[3] Britta Brügger,[2] Felix T. Wieland,[2]† John A. G. Briggs[1,4]†

Transport between compartments of eukaryotic cells is mediated by coated vesicles. The archetypal protein coats COPI, COPII, and clathrin are conserved from yeast to human. Structural studies of COPII and clathrin coats assembled in vitro without membranes suggest that coat components assemble regular cages with the same set of interactions between components. Detailed three-dimensional structures of coated membrane vesicles have not been obtained. Here, we solved the structures of individual COPI-coated membrane vesicles by cryoelectron tomography and subtomogram averaging of in vitro reconstituted budding reactions. The coat protein complex, coatomer, was observed to adopt alternative conformations to change the number of other coatomers with which it interacts and to form vesicles with variable sizes and shapes. This represents a fundamentally different basis for vesicle coat assembly.

Cellular transport vesicles are formed by conserved protein coats (*1*–*3*). Detailed structural information about vesicle coats assembled on a membrane bilayer has remained elusive. The clearest insights into the architecture of vesicle coats have been obtained by applying electron microscopy (EM) to coat protein complex COPII and clathrin protein cages, assembled in vitro from outer coat protein components in the absence of membranes (*1*, *4*, *5*). The cages have point group symmetries and discrete size distributions (*6*), whereas in vivo formed clathrin-